Title

The chemical convulsant diisopropylfluorophosphate (DFP) causes persistent neuropathology in adult male rats independent of seizure activity

Journal

Archives of Toxicology, 94(6)

ISSN

0340-5761

Authors

González, Eduardo A
Rindy, Alexa C
Guignet, Michelle A
et al.

Publication Date

2020-06-01

DOI

10.1007/s00204-020-02747-w

Peer reviewed

Archives of Toxicology
https://doi.org/10.1007/s00204-020-02747-w

ORGAN TOXICITY AND MECHANISMS

The chemical convulsant diisopropylfluorophosphate (DFP) causes persistent neuropathology in adult male rats independent of seizure activity

Eduardo A. González[1] · Alexa C. Rindy[1] · Michelle A. Guignet[1] · Jonas J. Calsbeek[1] · Donald A. Bruun[1] · Ashish Dhir[2] · Peter Andrew[1] · Naomi Saito[3] · Douglas J. Rowland[4] · Danielle J. Harvey[3] · Michael A. Rogawski[2] · Pamela J. Lein[1]

Received: 26 January 2020 / Accepted: 8 April 2020

Abstract

Organophosphate (OP) threat agents can trigger seizures that progress to *status epilepticus*, resulting in persistent neuropathology and cognitive deficits in humans and preclinical models. However, it remains unclear whether patients who do not show overt seizure behavior develop neurological consequences. Therefore, this study compared two subpopulations of rats with a low versus high seizure response to diisopropylfluorophosphate (DFP) to evaluate whether acute OP intoxication causes persistent neuropathology in non-seizing individuals. Adult male Sprague Dawley rats administered DFP (4 mg/kg, sc), atropine sulfate (2 mg/kg, im), and pralidoxime (25 mg/kg, im) were monitored for seizure activity for 4 h post-exposure. Animals were separated into groups with low versus high seizure response based on behavioral criteria and electroencephalogram (EEG) recordings. Cholinesterase activity was evaluated by Ellman assay, and neuropathology was evaluated at 1, 2, 4, and 60 days post-exposure by Fluoro-Jade C (FJC) staining and micro-CT imaging. DFP significantly inhibited cholinesterase activity in the cortex, hippocampus, and amygdala to the same extent in low and high responders. FJC staining revealed significant neurodegeneration in DFP low responders albeit this response was delayed, less persistent, and decreased in magnitude compared to DFP high responders. Micro-CT scans at 60 days revealed extensive mineralization that was not significantly different between low versus high DFP responders. These findings highlight the importance of considering non-seizing patients for medical care in the event of acute OP intoxication. They also suggest that OP intoxication may induce neurological damage via seizure-independent mechanisms, which if identified, might provide insight into novel therapeutic targets.

Keywords Diisopropylfluorophosphate · Micro-CT · Neurodegeneration · Organophosphate neurotoxicity · *Status epilepticus*

Abbreviations

AChE	Acetylcholinesterase
AS	Atropine sulfate
BChE	Butyrylcholinesterase
ChE	Cholinesterase
CT	Computed tomography
DFP	Diisopropylfluorophosphate
EEG	Electroencephalogram
FJC	Fluoro-Jade C

Eduardo A. González and Alexa C. Rindy contributed equally to this manuscript.

✉ Pamela J. Lein
pjlein@ucdavis.edu

[1] Department of Molecular Biosciences, University of California, Davis, School of Veterinary Medicine, 1089 Veterinary Medicine Drive, Davis, CA 95616, USA

[2] Department of Neurology, University of California, Davis, School of Medicine, 4860 Y Street, Sacramento, CA 95817, USA

[3] Department of Public Health Sciences, University of California, Davis, School of Medicine, One Shields Avenue, Davis, CA 95616, USA

[4] Center for Molecular and Genomic Imaging, University of California, Davis, College of Engineering, 451 Health Sciences Drive, Davis, CA 95616, USA

Published online: 18 April 2020

im	Intramuscular
ip	Intraperitoneal
OP	Organophosphate
2-PAM	Pralidoxime
PBS	Phosphate-buffered saline
ROI	Region of interest
sc	Subcutaneous
SE	Status epilepticus
T2w	T2-weighted
VEH	Vehicle

Introduction

Organophosphate (OP) nerve agents have been used as chemical threat agents in Tokyo and Syria (Okumura et al. 2005; Thiermann et al. 2013), and OP poisonings have been estimated to cause hundreds of thousands of deaths annually throughout the world (Gunnell et al. 2007). OPs cause acute neurotoxicity by inhibiting acetylcholinesterase (AChE), which can trigger seizures that progress to *status epilepticus* (SE), respiratory failure, and death (reviewed in Araujo et al. 2012). Clinical and epidemiological data suggest that humans who survive OP-induced SE exhibit persistent neurological deficits, such as structural brain damage, electroencephalographic abnormalities, cognitive deficits, and affective disorders (reviewed in Chen 2012). However, it has been observed that seizure behavior in humans acutely intoxicated with OPs is variable, ranging from the complete absence of apparent seizure activity to SE (Okumura et al. 1996; Peter et al. 2014). For example, victims of the Tokyo subway sarin attack exhibited differential susceptibility to cholinergic symptoms and seizure induction following acute exposure (Yanagisawa et al. 2006). While preclinical studies demonstrate that the severity and extent of brain damage following acute OP intoxication are proportional to seizure duration (Hobson et al. 2017; McDonough et al. 1995), it remains unclear whether intoxicated individuals who do not seize are susceptible to neurological damage.

Acute intoxication with the OP threat agent, diisopropylfluorophosphate (DFP), causes SE in experimental animals (Li et al. 2011; Todorovic et al. 2012) that results in acute and persistent neuropathology that parallels the neuropathology observed in humans following acute OP intoxication (Flannery et al. 2016; Guignet et al. 2019; Siso et al. 2017). However, over the past 10 years, we have observed that 10–15% of adult male Sprague Dawley rats exhibit minimal to no seizure behavior when injected with a dose of DFP that typically triggers prolonged seizure activity in rats of the same strain, sex, weight, and age. These observations are consistent with previous reports of variable sensitivity to DFP toxicity in Sprague Dawley rats (Russell et al. 1982), and of non-seizing animals in rodent models of acute intoxication with soman (Prager et al. 2013) or sarin (Lewine et al. 2018; Te et al. 2015).

A subpopulation of rats that are apparently resistant to DFP-induced seizures represents a unique model for determining whether acute OP intoxication can induce neurological damage in non-seizing individuals. Here, we leveraged this subpopulation to compare seizure behavior, electrographic seizure activity, AChE activity, and neuropathology in rats that respond to acute DFP intoxication with robust seizure behavior versus those that exhibit minimal seizure behavior. Our findings suggest that DFP can cause persistent neurological damage independent of severe seizure activity. In addition, our results indicate that while seizure activity influences the spatiotemporal profile and magnitude of the neuropathologic response to acute OP intoxication, it is not the sole determinant of persistent OP neurotoxicity. These data suggest that therapeutic strategies focused solely on terminating seizure activity will likely not fully protect the brain against long-term neurological damage. Understanding seizure-independent mechanisms of damage may provide novel therapeutic insights for mitigating adverse neurological outcomes in all exposed individuals in a chemical emergency involving OPs.

Materials and methods

Animals and husbandry

Animals were maintained in facilities fully accredited by AAALAC International, and all studies were performed with regard for alleviation of pain and suffering under protocols approved by the UC Davis Institutional Animal Care and Use Committee (IACUC protocol numbers 20122 and 20165). All animal experiments were conducted in accordance with the ARRIVE guidelines and the National Institutes of Health guide for the care and use of laboratory animals (NIH publication No. 8023, revised 1978). All surgical procedures were performed under the UC Davis IACUC guidelines for rodent survival surgery. Adult male Sprague Dawley rats (~ 8 weeks old, 250–280 g; Charles River Laboratories, Hollister, CA, USA) were housed individually in standard plastic cages under controlled environmental conditions (22 ± 2 °C, 40–50% humidity) with a normal 12-h light/dark cycle. Food and water were provided ad libitum.

Animal selection

For ~ 10 years, the Lein lab has been regularly conducting experiments with rats acutely intoxicated with DFP. Over the first few years, we began to notice that a small percentage of animals did not exhibit a robust seizure behavioral response following injection with DFP. To determine the approximate

frequency of DFP low responders, historical seizure data from several cohorts (combined total of 62 animals) were evaluated retrospectively. Due to the low incidence of DFP low responders, the animals reported here were removed from various cohorts over a period of ~ 4 years. This was done primarily because of ethical concerns associated with generating a single large animal cohort to study only a small subset of animals. When a DFP low responder was identified in an ongoing study, a DFP high responder and vehicle control were randomly selected from the same cohort to control for differences across cohorts. The animals removed from the original cohort for this study were analyzed exclusively for the present study. Therefore, none of the animals reported herein have been analyzed in another study nor have data from these animals been previously published. Animals were selected over a 4-year period until sample sizes for each endpoint reached the number needed to reliably detect group differences as determined by power analysis (e.g., geometric mean ratios of 2.0 + under two-sided testing with alpha = 5%). As described in Table 1, unique cohorts of animals were collected for electroencephalographic (EEG) recordings because electrode implantation is a confound for histological analyses. Another unique cohort was used for micro-computed tomography (micro-CT) because it was performed at a late time point and required a higher sample size as determined by power analysis.

Dosing paradigm

Upon arrival in the laboratory, DFP (Sigma Chemical Company, St Louis, MO, USA) was aliquoted and stored at − 80 °C. Under these storage conditions, DFP remains stable for 1 year (Heiss et al. 2016). The purity of each lot of DFP was determined in-house using ^{1}H-, ^{13}C, ^{19}F and ^{31}P-NMR methods, as previously described (Gao et al. 2016), and found to be approximately 90 ± 7%. For all experiments, DFP was diluted with ice-cold sterile phosphate-buffered saline (PBS, 3.6 mM Na_2HPO_4, 1.4 mM NaH_2PO_4, 150 mM NaCl; pH 7.2) five min before administration. Unanesthetized rats were injected sc in the subscapular region with 300-µl DFP at 4 mg/kg, a dose shown to induce *status epilepticus* in adult male Sprague Dawley rats (Flannery et al. 2016; Guignet et al. 2019). To increase survival following DFP exposure, animals were injected im with 2 mg/kg atropine sulfate (Sigma) and 25 mg/kg pralidoxime (2-PAM; Sigma) in sterile isotonic saline (0.9% NaCl) within 1 min after DFP injection (Fig. 1a). Certificates of analysis provided by the manufacturers confirmed the purity of atropine sulfate (> 97%, lot #BCBM6966V) and 2-PAM (> 99%, lot #MKCG3184). These drugs effectively block peripheral cholinergic toxicity, thereby reducing mortality (Bruun et al. 2019). Vehicle (VEH) control animals were injected sc with 300-µl ice-cold sterile PBS in place of DFP but were similarly treated with atropine and 2-PAM. A random number generator was used to assign animals to experimental groups. Once returned to their home cage, rats were given access to moistened chow for 3–5 days or until they resumed consumption of solid chow. All experiments were performed in at least three independent cohorts.

Behavioral seizure scoring

To identify animals with "high" versus "low" seizure activity, seizure behavior was scored every 5 min during the first 120 min after DFP injection and then every 20 min from 120–240 min post-DFP injection using an established seizure behavior scale (Deshpande et al. 2010) as previously described (Guignet et al. 2019). The seizure scores for each individual animal were averaged over the first 4 h post-injection to determine the "average seizure score". An average seizure score of 2.5 was used as the threshold to separate animals that exhibited behavior consistent with SE (referred to as "DFP high responders") and animals that did not exhibit behavior consistent with SE (referred to as "DFP low responders").

Table 1 Summary of animal cohorts

Cohort	Endpoint(s) evaluated	Sample size	Figures
Historical	Frequency of DFP low responders	62 DFP rats	1b
1	Seizure behavior Cholinesterase activity FluoroJade-C (neurodegeneration)	16/group 4–6/group used for cholinesterase activity 6–10/group used for FluoroJade-C	1d 4 5
2	Acute EEG (1 h post-DFP)	6–7/group	2
3	Long-term EEG (24 h post-DFP)	3–4/group	3
4	Micro-CT	3 Vehicle 14 DFP low responders 6 DFP high responders	6

EEG electroencephalogram

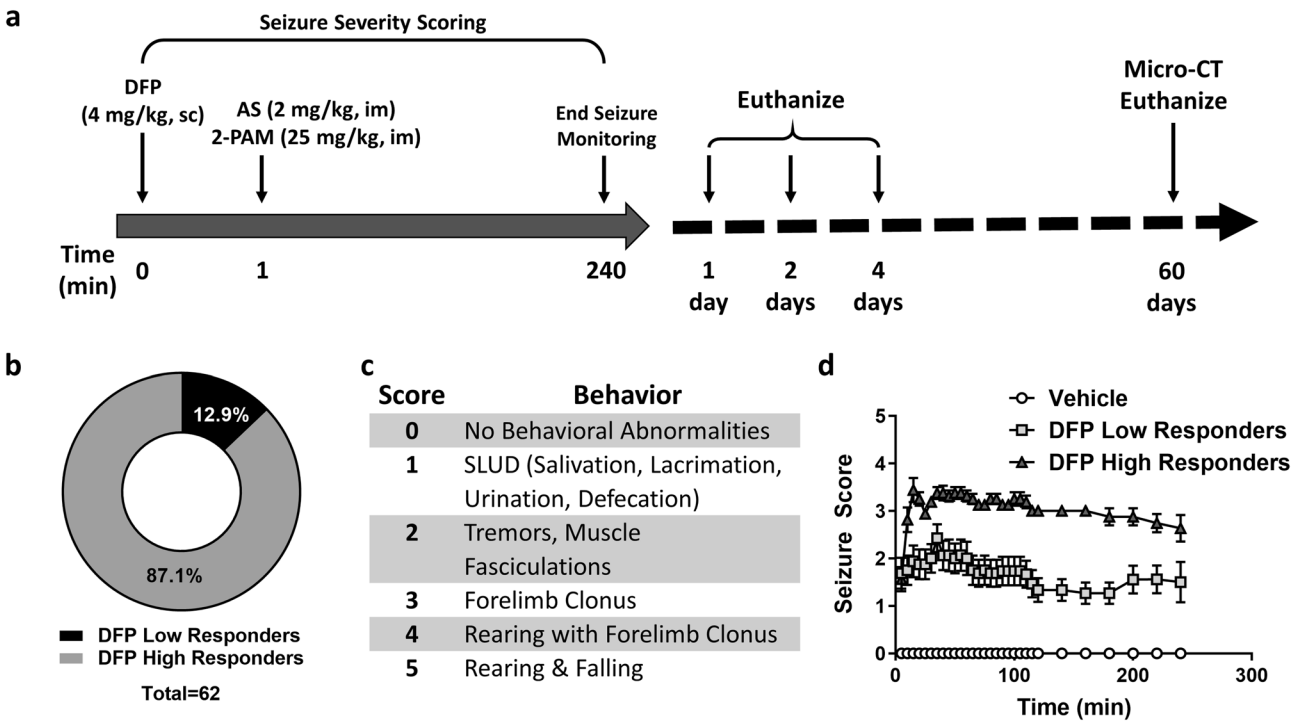

Fig. 1 The rat model of acute DFP intoxication and seizure behavior of DFP low versus high responders. **a** Schematic illustrating the dosing paradigm used to trigger DFP-induced seizures in adult male Sprague Dawley rats and time-line of data collection. **b** Percentage of DFP low vs. high responders in previous studies in the Lein lab. Of 62 DFP-intoxicated rats, 54 were high responders and eight were low responders. **c** Scale used to score seizure behavior in DFP-intoxicated rats. Rats with an average seizure score of ≤ 2.5 were identified as "DFP low responders". **d** Temporal profile of seizure scores in VEH, DFP low responders, and DFP high responders. Data presented as mean ± SE ($n = 16$ animals/group)

EEG recordings

In an independent cohort of animals not used for biochemical or histological analyses, both DFP low and high responders (6–7 per group) were monitored for 1 h post-DFP to determine whether behavioral seizures correlated with electrographic seizure activity. A tethered EEG system was used for these short-term electrographic experiments as previously described (Guignet et al. 2019). Briefly, 60 mg/kg ketamine and 0.5 mg/kg dexmedetomidine were injected ip to anesthetize animals and stabilize them in a stereotaxic apparatus (Kopf Instruments, Tujunga, CA, USA). Six recording screws were implanted epidurally and connected to a 6-pin rat implant (Pinnacle 8239-SE3, Pinnacle Technology, Lawrence, KS, USA). Animals were allowed a minimum of 7 days to recover from surgery before undergoing further procedures. EEG recordings were acquired for ~ 10 min prior to DFP injection (baseline period) and for 1 h post-DFP injection using the Pinnacle 8401 Data Conditioning & Acquisition System (Pinnacle Technology). These data were reviewed using Sirenia Seizure Pro software (Pinnacle Technology) and quantitated using NeuroScore™ (version 3.3.9, Data Sciences International, St. Paul, MN, USA). EEG data were filtered using a band-pass filter of 20–70 Hz to reduce noise, as previously described (Pouliot et al. 2016), and analyzed using epoch durations of 1 s. Spike amplitude was quantified for each time period using root mean squared (RMS) values automatically extracted from the band-pass-filtered EEG traces. To calculate spike frequency, the average amplitude of the baseline period was calculated for each animal (~ 20 µV in most animals). Peaks that reached > 2 × baseline amplitude were identified as paroxysmal and, therefore, quantified. The spike frequency (number of peaks/s above baseline) and spike amplitude (RMS) were quantified and averaged over the 1-h recording period.

To determine whether DFP low responders exhibit delayed electrographic abnormalities, a different cohort of animals (3–4 per group) was implanted with cortical electrodes to wirelessly monitor electrographic activity for 24 h following acute DFP intoxication. Animals were deeply anesthetized with isoflurane (1–3%) in medical grade oxygen (flow rate = 1L/min) for the entire duration of the surgical procedure. Fur was shaved from the surgical site before stabilizing the head in a stereotaxic apparatus (Stoelting, Wood Dale, IL, USA). Altalube™ ophthalmic ointment (Altaire Pharmaceuticals Inc, Riverhead, NY, USA) was applied to

the eyes to prevent them from drying out during the procedure. A complete aseptic surgical scrub of the skin was performed using three alternating rounds of betadine scrub (Purdue Products, Stamford, CT, USA) and 70% isopropyl alcohol wipes (Covidien Plc, Dublin, Ireland) before creating an approximate 1.5-inch incision that extended from between the eyes to the base of the skull. Four head mount screws were implanted at the following coordinates relative to Bregma: 2 mm anterior, 7 mm posterior, and 1.5 mm laterally on each side of the sagittal skull suture. Sterile F20-EET telemetry devices (Data Sciences International) were inserted between the skin and muscle layer along the flank of the animal, and the recording wires were extended to the skull and secured around the head mount screws. The screws and leads were secured using dental cement (Stoelting). The incision site was sutured (Ethicon, Bridgewater, NJ, USA) over the head mount, and animals were given separate injections of 5% dextrose in sterile saline (1 mL, sc, Baxter Healthcare, Deerfield, IL, USA) and meloxicam (4 mg/kg, sc, Vet One, Boise, ID, USA) before being removed from anesthesia and allowed to recover on a heating pad. Animals were administered two additional doses of meloxicam (4 mg/kg, sc, once daily for 48 h) and allowed to recover for 14 days before being administered DFP.

One day prior to injection with DFP, animals were placed in their home cages on wireless PhysioTel® Receivers (Model RPC1, Data Sciences International). Baseline electrographic activity (Ponemah software version 5.32, Data Sciences International) coupled with video monitoring (Noldus media recorder, version 2.6, Wageningen, Netherlands) was recorded for a full 24 h to capture normal wake and sleep EEG patterns in freely moving animals. On the day of DFP injections, animals were given either a single dose of DFP or VEH (PBS), and video EEG activity was recorded during the first 24 h after DFP administration. Seizure activity was determined as spike wave discharges with an amplitude at least twice that of background activity in awake animals with at least 100-Hz frequency and duration of at least 5 s. All seizures were automatically detected using NeuroScore™ (version 3.3.9, Data Sciences International) and manually validated by a trained investigator.

Cholinesterase assays

At 1 and 4 days post-DFP exposure, animals were anesthetized with 4–5% isoflurane in medical grade oxygen (Western Medical Supply, Arcadia, CA, USA) and euthanized by perfusion with cold PBS (15 mL/min) using a Masterflex peristaltic pump (Cole Parmer, Vernon Hills, IL, USA). Brains were rapidly harvested and brain regions rapidly dissected on ice. The cortex, hippocampus, and amygdala of each animal were snap frozen on dry ice and stored at − 80 °C. The Ellman assay (Ellman et al. 1961) was used to measure cholinesterase activity in each brain region using 5,5′-dithio-bis(2-nitrobenzoic acid) (DTNB, Sigma) as the colorimetric reagent and acetylthiocholine iodide (ASChI, Sigma) as the AChE substrate. All samples were homogenized in lysis buffer (0.1-M phosphate buffer, pH 8.0 with 0.1% Triton) using a Polytron PT 1200 E and centrifuged for 1 min at 13,400×*g*. Supernatant was collected and plated in triplicate in a 96-well plate for analysis. Blank wells contained an equal volume of buffer with DTNB. After equilibration with DTNB for 5 min, the reaction was started with the addition of ASChI. ASChI hydrolysis was quantified by measuring changes in absorbance at 405 nm over 15 min using the Synergy H1 Hybrid Plate Reader with Gen5 2.0 software (BioTek Instruments, Winooski VT, USA). All samples were run in the absence and presence of the butyrylcholinesterase (BChE) inhibitor tetraisopropyl pyrophosphoramide (100 µM) to measure total ChE versus AChE-specific activity, respectively. ChE activity was normalized against total protein concentration determined using the BCA assay according to the manufacturer's directions (Pierce, Rockford, IL, USA).

Fluoro-Jade C staining

At 1, 2, 4, and 60 days post-DFP exposure, animals were anesthetized with 4–5% isoflurane in medical grade oxygen and perfused with cold PBS (15 mL/min) using a Masterflex peristaltic pump ($n = 6$–10/group). Brains were quickly harvested, cut into 2-mm-thick coronal sections starting at Bregma point 0 and post-fixed in cold 4% (w/v) paraformaldehyde (Sigma) in PBS (pH 7.4) for 24 h. Coronal sections were removed from fixative, cryoprotected in 30% (w/v) sucrose (Fisher, Houston, TX, USA) in PBS overnight at 4 °C, and then embedded in OCT medium (Fisher) in plastic cryomolds and stored at − 80 °C until sectioned. Frozen blocks were cryosectioned into 10-µm-thick coronal sections, which were mounted on Superfrost Plus microscope slides (Fisher) and stored at − 80 °C until stained. Fluoro-Jade C (FJC; Cat. #AG325, Lot #2301303, Millipore, Billerica, MA, USA) labeling was performed according to the manufacturer's protocol with minor modifications. Briefly, after 30 min of drying at 50 °C, sections were rinsed with 70% ethanol and incubated for 10 min on a shaker table in a solution of 0.06% (w/v) potassium permanganate (Sigma) in distilled water followed by 2 min in distilled water. Sections were then incubated for 10 min in a freshly prepared solution of 0.0001% FJC in 0.1% (v/v) acetic acid (Acros Organics, Geel, Belgium) in distilled water containing a 1:50,000 dilution of DAPI (Invitrogen, Carlsbad, CA, USA). The slides were dried completely at 50 °C and then dipped in xylene (Fisher) for 1 min. The slides were mounted in Permount (Fisher), cover slipped, dried overnight, and stored at 4 °C until imaged.

Images were automatically acquired at 20X magnification using the ImageXpress high content imaging system (Molecular Devices, Sunnyvale, CA, USA). The number of FJC-labeled cells per unit area was automatically quantified in the somatosensory cortex, hippocampus, piriform cortex, and thalamus using the Cell Counter plugin for the ImageJ image analysis software (version 1.50i, https://imagej.nih.gov/ij). Input parameters for determining cell size and circularity were 50–150 µm diameter and 0.3–1.0 circularity, respectively. Four brain sections with Bregma ranging from − 2 to − 5 mm were analyzed per animal. FJC-labeled cells were counted in three regions per section, and the number of cells was averaged across sections in each brain region per animal. The number of FJC-labeled cells was quantified as the number of positively labeled cells per 1.0 mm^2. Image acquisition and analysis were performed by an investigator blinded to experimental group.

Micro-CT imaging

Animal brains were imaged in vivo at the UC Davis Center for Molecular and Genomic Imaging using an Inveon MM CT scanner (Siemens Preclinical Solutions, Malvern, PA, USA). Animals were anesthetized with isoflurane/O_2 (Piramal Healthcare, Bethlehem, PA, USA) using 2.0–3.0% (vol/vol) to induce and 1.0–2.0% (vol/vol) to maintain anesthesia. Once animals were completely anesthetized, as determined by a complete absence of toe squeeze reflex, they were stereotactically restrained within the CT scanner on custom restraint beds. Scans were digitally reconstructed using a Fledkamp algorithm with Shepp-Logan filter into 16-bit values.

Micro-CT scan images were analyzed using Amira software (version 6.5.0, ThermoFisher). Briefly, regions of interest (ROIs) were drawn around the dorsolateral and medial thalamus on previously acquired T2-weighted (T2w) magnetic resonance images. Micro-CT scans were "de-noised", manually aligned to T2w images, and an intensity threshold was applied to isolate areas of mineralization. ROI volumes were exported from Amira for the dorsolateral thalamus, medial thalamus, and mineral deposits. All analyses were conducted by a single experimenter without any knowledge of exposure group and time point. The percent mineralization was calculated for each ROI, and three-dimensional reconstructions of the mineralized areas in both the dorsolateral and medial thalamus were combined to visualize mineral deposits throughout the thalamus. While this technique provides clear visualization of mineralized tissues, microCT does not provide identification of the chemical composition of mineral deposits.

Statistical analysis

Primary outcomes included measures of total ChE, AChE, and number of FJC-labeled cells across multiple regions of the brain for three groups of animals (VEH, DFP low responders, and DFP high responders). The ChE measures were obtained for the cortex, hippocampus, and amygdala. The number of FJC-labeled cells was measured across the somatosensory cortex, hippocampus, piriform cortex, and thalamus. Mixed-effects regression models, including animal-specific random effects, were used to assess the differences between the groups across the brain regions. Because time was another factor of interest, groups were further split by day (ChE: days 1, 4; FJC labeling: days 1, 2, 4, 60). Exploratory analysis indicated that a natural logarithmic transformation was needed for all outcomes to stabilize the variance and meet the underlying assumptions of the mixed-effects models. Due to zeros in the FJC-labeling experiments, all FJC values were shifted by 5 prior to the log-transformation. Days, group, and brain region were all variables of interest in the models. Interactions between these variables were also considered. Akaike information criterion was used for model selection, and Wald tests were used for comparing groups in each brain region by time point.

Micro-CT data were available for 23 animals for two regions (medial and dorsolateral thalamus). Mixed-effects regression models, including animal-specific random effects, were used to assess differences between groups. Exploratory analysis indicated that a natural logarithmic transformation was needed for percent mineralization to stabilize the variance and meet the underlying assumptions of the mixed-effects models. Due to observed zeroes for this outcome, all values were shifted by 0.5 prior to taking the natural logarithm. Primary factors of interest included group (VEH, DFP low responders, and DFP high responders) and region (medial and dorsolateral thalamus). An interaction between these variables was also considered. Akaike information criterion was used for model selection to identify the best model. Specific contrasts were constructed for all pairwise comparisons between groups and examined using Wald tests.

FJC and micro-CT results are presented as geometric mean ratios. These ratios may be interpreted as fold changes, so that a ratio of 1.5 corresponds to a 50% increase and a ratio of 0.5 corresponds to a 50% decrease. Point estimates of the ratios and the 95% confidence intervals are presented in the figures. When the confidence interval includes 1, there is no statistical evidence of a difference between groups. However, when the confidence interval does not include 1, the estimated effect is significant at the 5% level. All analyses were conducted using SAS version 9.4, and graphics were created in R version 3.1.0.

Results

DFP low responders do not exhibit seizure-like behavior or electrographic activity

Historic data in the Lein laboratory suggest that ~ 13% of adult male Sprague Dawley rats exposed to a DFP dosing paradigm that typically generates robust seizures (Fig. 1a) do not respond with seizure-like behavior (Fig. 1b). To determine whether animals that do not show overt seizure behavior develop neurological consequences, we selected DFP low responders as they were identified in ongoing studies in the lab for further study. A vehicle control and DFP high responder was randomly selected from each cohort of animals from which DFP low responders were obtained, resulting in 16 animals per group collected over a 2-year period. To identify DFP low vs. high responders, we used a modified Racine scale [(Deshpande et al. 2010); also see Fig. 1c] to assess seizure behavior (Fig. 1d). The mean ± SE of the average seizure score across all DFP low responders was 1.7 ± 0.3. Notably, none of the animals in this group exhibited seizure behavior scores above 2.5 throughout the first 4 h post-exposure. The mean ± SE of the average seizure score across all DFP high responders was 3.1 ± 0.2. Vehicle controls (animals not exposed to DFP) did not exhibit any seizure behavior or any signs of cholinergic toxicity; thus, their mean seizure score was 0.

To confirm the absence of seizure activity in DFP low responders, a separate cohort of animals was implanted with intracortical electrodes to record EEG activity during the first 60 min post-DFP. EEG recordings showed comparable baseline activity between DFP high and low responders (Fig. 2a). However, following acute DFP intoxication, the EEG of DFP high responders was consistent with SE, while the EEG of DFP low responders did not appear different from baseline. Quantification of spike amplitude and frequency confirmed there was no significant difference between baseline EEG in high vs. low responders (Fig. 2b). Following DFP administration, high responders showed significantly greater spike amplitude and frequency than DFP low responders. Correlation analysis of all DFP animals (including both high and low responders) revealed that behavioral seizure scores are strongly correlated with EEG measures (Fig. 2c), including spike amplitude (left; Spearman $r = 0.780$, $p = 0.002$) and spike frequency (right; Spearman $r = 0.835$, $p = 0.0006$).

To determine whether DFP low responders develop delayed seizure activity, EEG recordings were collected from both DFP high and low responders over the first 24 h post-injection (Fig. 3a). DFP high responders showed ~ 60 min of total seizure activity compared to 0 min in DFP low responders (Fig. 3b). Both DFP high and low responders showed comparable baseline electrographic activity for ~ 2 h prior to DFP injection (Fig. 3c). EEG traces over the 24-h recording period showed peak seizure activity in DFP high responders at 30 min, with paroxysmal spike activity at 6 h post-exposure. Although there was a dramatic reduction in seizure activity in the DFP high responders by 12 h, abnormal spike activity was observed throughout the 24-h period. In contrast, DFP low responders had minimal deviation from baseline EEG activity throughout the 24-h recording period (Fig. 3c).

Both DFP high and low responders show significant cholinesterase inhibition

A possible explanation for the lack of seizure activity in DFP low responders relative to DFP high responders is differences in DFP metabolism and uptake in the brain. Thus, cholinesterase activity was measured in the cortex, hippocampus, and amygdala at 1 and 4 days post-exposure. Relative to VEH animals, DFP low responders had significantly decreased activity of total ChE and AChE in all brain regions at both time points (Fig. 4). Similarly, total ChE and AChE activities were significantly decreased in all brain regions of DFP high responders at both time points compared to VEH animals. Comparative analysis suggests that total ChE and AChE activities were similarly inhibited in DFP low and high responders in all brain regions examined, suggesting no differences in DFP metabolism or brain uptake between the two groups.

Acute DFP intoxication triggers neuronal degeneration in DFP low and high responders

FJC staining was performed at both early (1, 2, and 4 days) and late (60 days) times post-DFP injection to evaluate neurodegeneration in brain regions previously found to be significantly affected by acute DFP intoxication, specifically, the somatosensory cortex, hippocampus, piriform cortex, and thalamus (Hobson et al. 2017; Siso et al. 2017). Representative photomicrographs of FJC staining in the somatosensory cortex of VEH, DFP low responders, and DFP high responders (Fig. 5a) reveal negligible FJC staining in VEH animals at any time point, and significantly increased FJC staining in DFP high responders as early as 1 day post-exposure that persists at 60 days post-exposure. An increase in FJC-labeled cells was also evident in the somatosensory cortex of DFP low responders, although this appeared to be delayed and of lower magnitude compared to the DFP high responders.

Quantitative assessment of the number of FJC-labeled cells in the somatosensory cortex, hippocampus, piriform cortex, and thalamus as a function of time post-exposure confirmed these observations (Fig. 5b). The number of

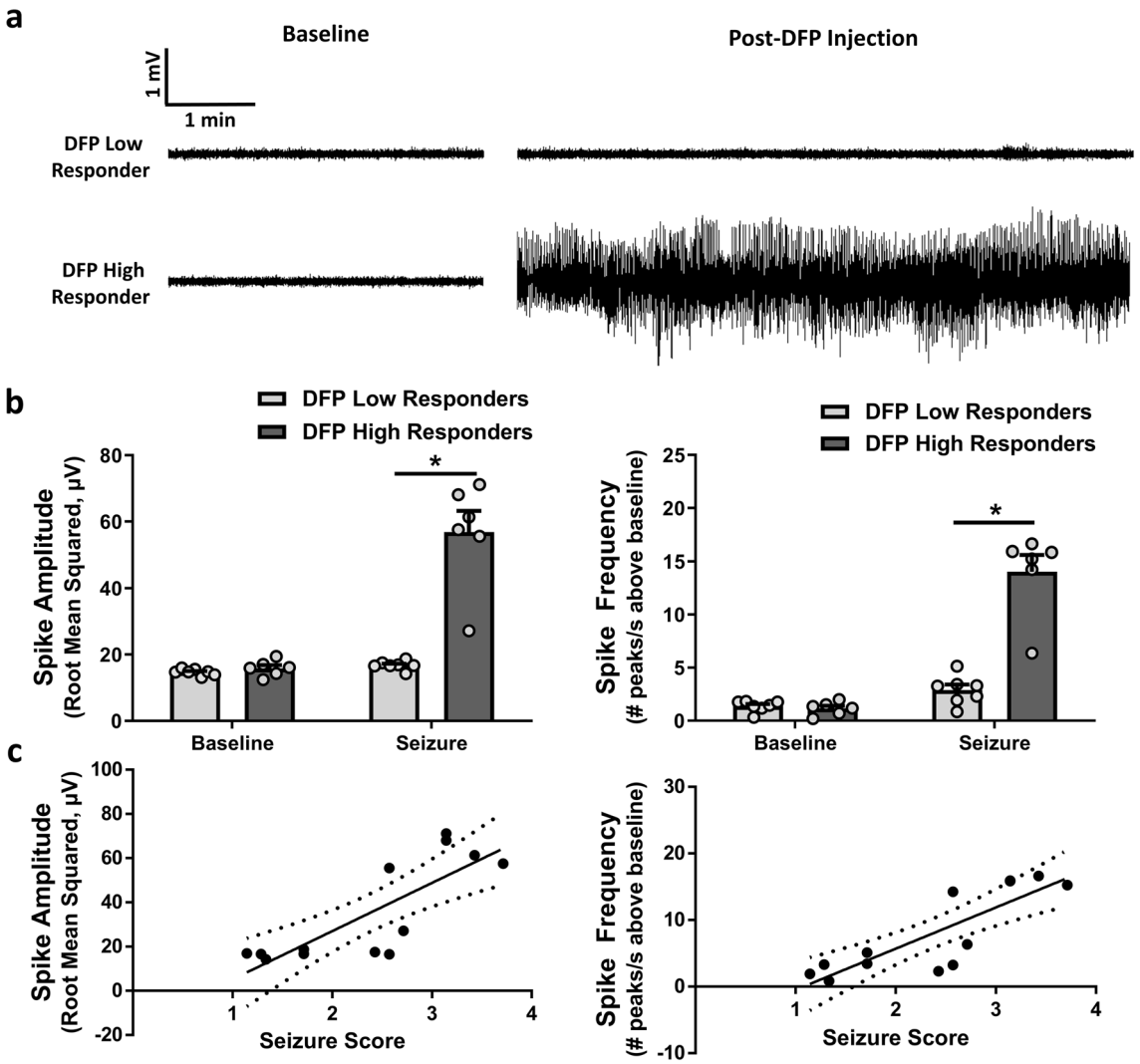

Fig. 2 Behavioral seizure scores correlate with electrographic activity during the first 60 min post-DFP. **a** Representative EEG traces in high and low responding animals before DFP injection (baseline period) and within the first 60 min post-intoxication. **b** Quantitative assessment of spike amplitude and spike frequency in both DFP high and low responding animals at baseline and within the first 60 min post-DFP intoxication. Group data are shown with bars representing the mean ± standard error of the mean ($n = 6$–7 animals/group). *Significantly different at $p < 0.05$. **c** Correlation analysis between seizure score and spike amplitude (left; Spearman $r = 0.780$, $p = 0.002$) and between seizure score and spike frequency (right; Spearman $r = 0.835$, $p = 0.0006$)

FJC-labeled cells in DFP low responders did not differ from VEH animals in any brain region at 1 day post-exposure, except for a slight increase in the piriform cortex ($p = 0.03$). However, on days 2 and 4 post-exposure, DFP low responders had significantly increased numbers of FJC-labeled cells in all four brain regions relative to VEH. By day 60 post-exposure, FJC staining in DFP low responders was not significantly different from that in VEH in any brain regions, except the piriform cortex. In contrast, relative to VEH, DFP high responders had significantly increased numbers of FJC-labeled cells in all four brain regions at 1, 2, and 4 days post-exposure. By day 60 post-exposure, significantly elevated FJC staining was only apparent in the somatosensory cortex of the DFP high responders ($p = 0.002$). The number of FJC-labeled cells was significantly greater in DFP high responders relative to DFP low responders in all four brain regions on days 1 and 2 post-exposure. This difference persisted on days 4 and 60 post-exposure in the somatosensory cortex, but not in the hippocampus, piriform cortex, or thalamus.

DFP low and high responders show significant mineralization in the thalamus at 60 days post-exposure

Calcium dysregulation is known to occur following acute OP intoxication (Deshpande et al. 2016), and calcification

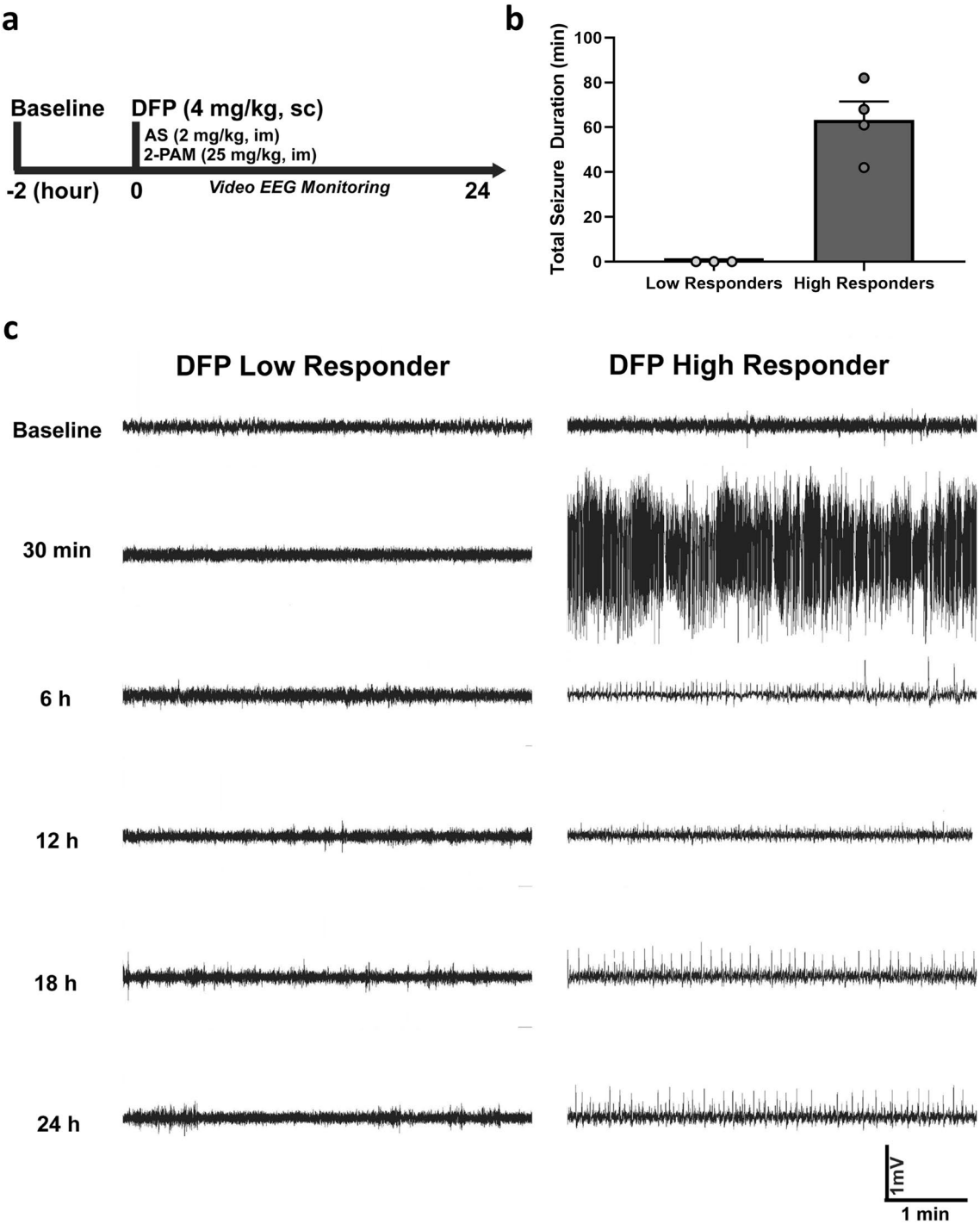

Fig. 3 DFP low responders show no electrographic evidence of seizure activity during the first 24 h post-intoxication. **a** Experimental timeline for evaluation of seizure activity in EEG-implanted animals during the first 24 h following DFP intoxication. **b** Quantitative assessment of the total duration of electrographic seizure activity (min) during the first 24 h post-DFP in high responding (dark gray; $n=4$) and low responding (light gray; $n=3$) animals. Data presented as mean ± SD; $p=0.0571$ as determined by Mann–Whitney test. **c** Representative EEG traces in high responding (right) and low responding (left) DFP animals at baseline, 30 min, 6 h, 12 h, 18 h and 24 h post intoxication

in the brain is associated with numerous neurologic conditions, including chemical-induced SE (Aggarwal et al. 2018; Gayoso et al. 2003). Therefore, micro-CT was used to assess mineralization in the brain of DFP rats. Significant mineralization was detected in both the medial thalamus and dorsolateral thalamus of DFP low and high responders at 60 days

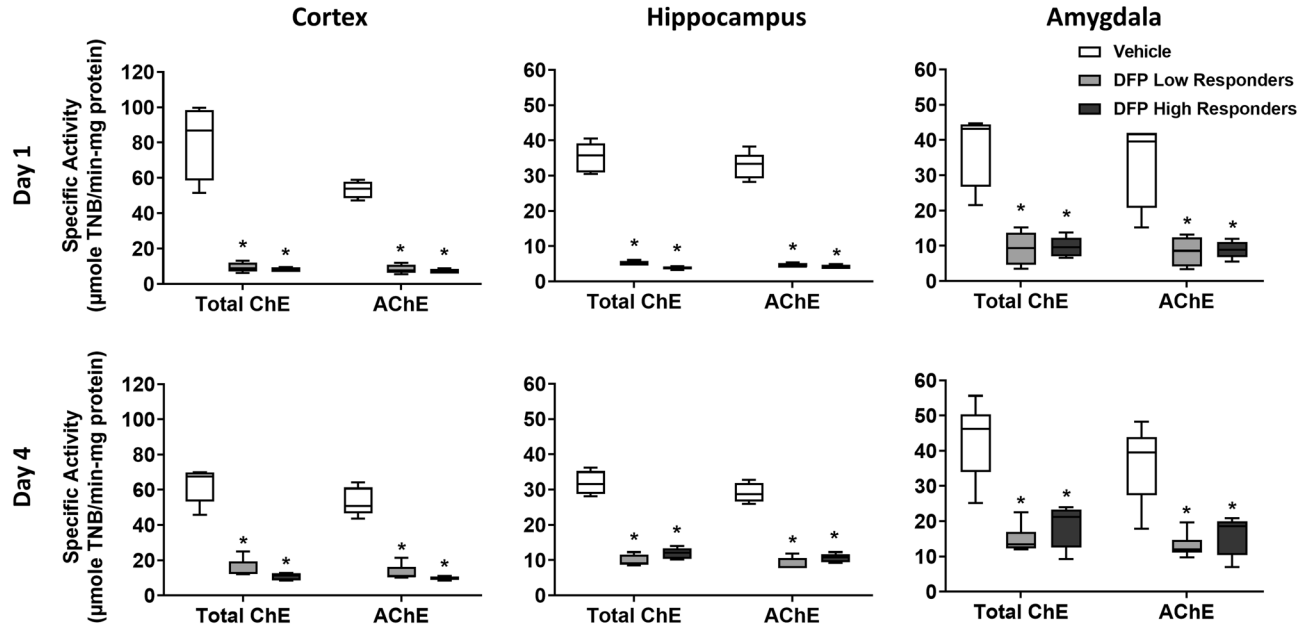

Fig. 4 Cholinesterase activity in the brain is significantly and similarly inhibited in low and high responding DFP animals. The specific activity of total cholinesterase (total ChE) and acetylcholinesterase (AChE) was measured in cortical, hippocampal, and amygdalar tissue at 1 day and 4 days post-DFP injection. Group data are shown with boxes representing the 25–75 percentiles; horizontal lines in the boxes, the median; and whiskers, the maximum and minimum values ($n = 4$–6 VEH, 5–8 DFP animals). *Significantly different from vehicle at $p < 0.05$

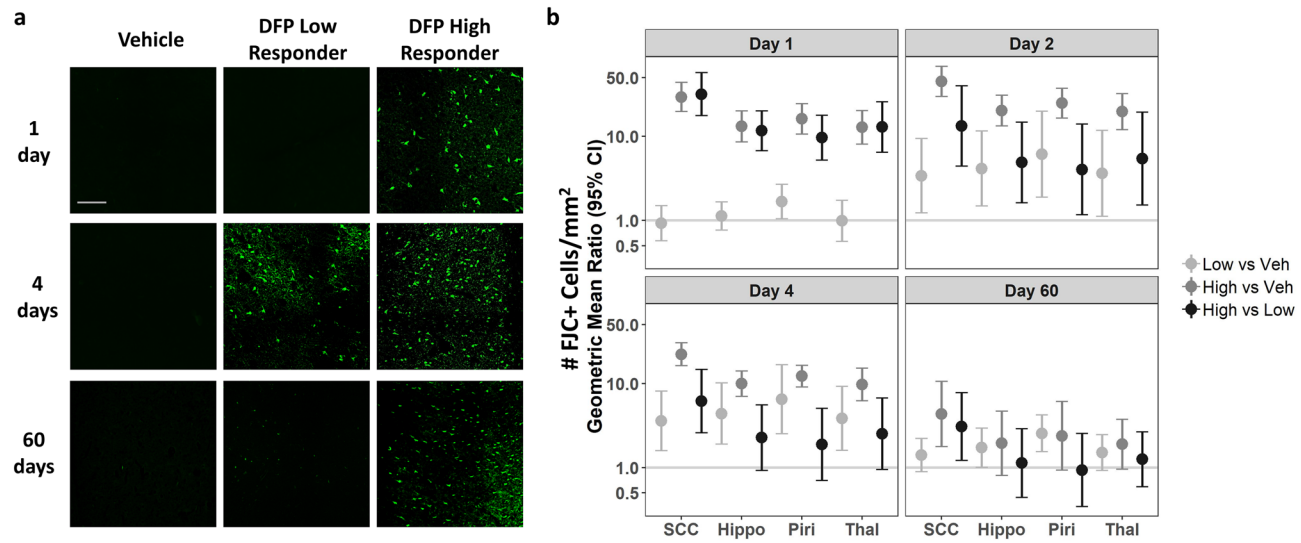

Fig. 5 Low and high responding DFP animals exhibit significant neurodegeneration in multiple brain regions. **a** Representative photomicrographs of FluoroJade-C (FJC) staining in the somatosensory cortex of vehicle controls, DFP low responders, and DFP high responders at 1, 4, and 60 days post-exposure. Bar = 100 µm. **b** The number of FJC-labeled cells was quantified in the somatosensory cortex (SSC), hippocampus (Hippo), piriform cortex (Piri), and thalamus (Thal) of vehicle controls (VEH), DFP low responders, and DFP high responders at 1, 2, 4, and 60 days post-DFP injection. Data shown as the geometric mean ratio with 95% confidence intervals. Confidence intervals entirely above 1 indicate a significant difference between the two groups being compared at $p < 0.05$ ($n = 6$–10 animals/group)

post-DFP exposure (Fig. 6a, b). Quantification of the percent mineralization within the region of interest confirmed significantly increased mineralization in the thalamus of both DFP low and high responders compared to VEH animals (Fig. 6c). However, there was no significant difference in the percent area of mineralization in the thalamus of DFP

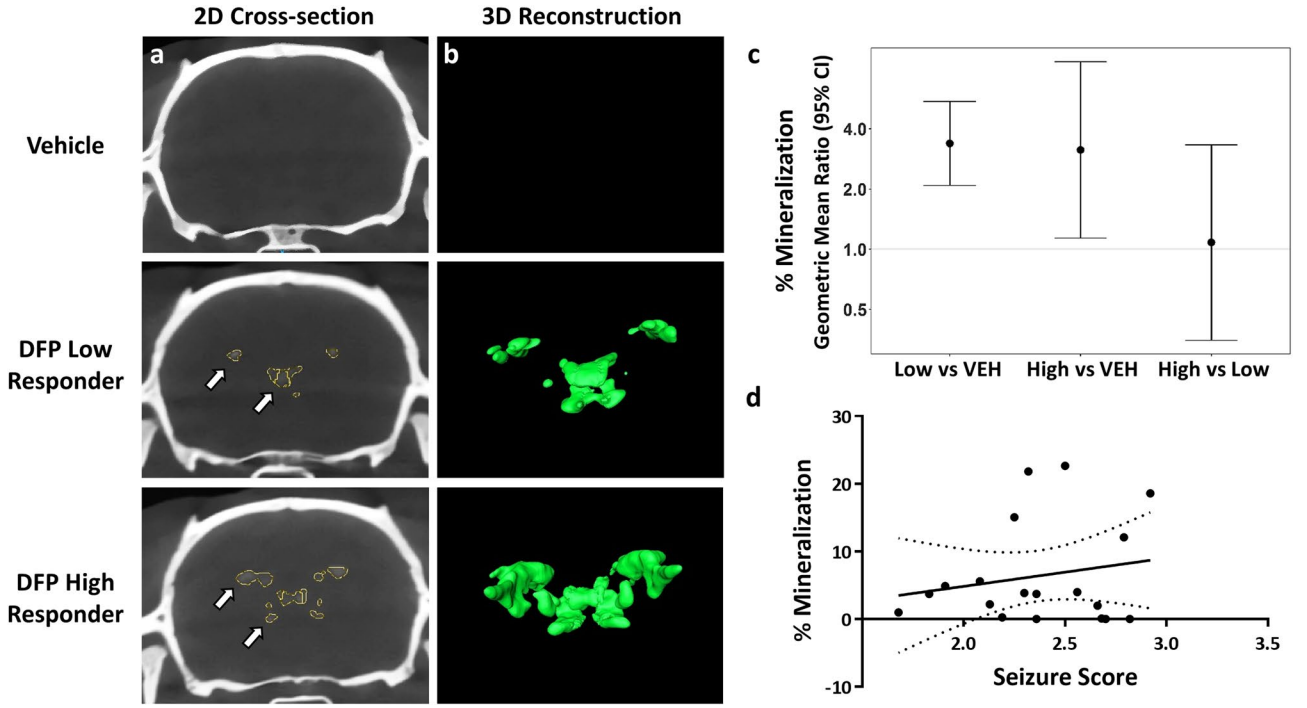

Fig. 6 DFP low and high responders have significant mineralization in the thalamus at 60 days post-exposure. **a** Representative two-dimensional (2D) whole brain micro-CT output images. Mineralized areas were automatically detected (yellow outline). Arrows point to representative mineral deposits. **b** 3D micro-CT images generated from the 2D output images showing mineral deposits (green) in the brains of vehicle, DFP low responding, and DFP high responding animals. **c** Quantification of the percent mineralized area relative to total brain region volume in the medial thalamus and dorsolateral thalamus of vehicle (VEH), DFP low responding, and DFP high responding animals. Statistical significance between groups did not vary by brain region, so all reported differences apply to both the medial thalamus and dorsolateral thalamus. Data are represented as the geometric mean ratio with 95% confidence intervals. Confidence intervals entirely above 1 indicate a significant difference between the two groups being compared at $p < 0.05$ ($n = 3$ VEH, 6–14 DFP animals). **d** Correlation analysis between seizure score and percent mineralization in the brain. Spearman $r = 0.189$, $p = 0.43$

high vs. low responders. Correlational analysis of all DFP-intoxicated animals (low and high responders) failed to find a correlation between average seizure score and percent area of mineralization (Spearmen $r = 0.189$, $p = 0.43$) (Fig. 6d).

Discussion

Previous reports have demonstrated that repeated exposure to lower doses of DFP (400 µg/kg) that do not trigger seizures can cause neuronal injury and behavioral changes in a rodent model (Phillips and Deshpande 2016). Here, we extend these observations by demonstrating that a single exposure to DFP at a dose that elicits robust SE in the majority of exposed animals can also cause neurological damage independent of seizure activity. Our findings highlight the importance of considering neuropathological consequences in both seizing and non-seizing individuals following acute OP intoxication.

As summarized in Table 2, DFP low responders show little to no seizure activity, despite > 80% inhibition of brain AChE, which is well above the threshold of > 65% AChE

Table 2 Summary of major findings

Group	Avg. Seizure Score	EEG activity	Cholinesterase inhibition	FluoroJade C staining	Brain mineralization
Vehicle	0	–	–	–	–
DFP Low	1.7	–	+ + +	+ + (delayed)	+ + +
DFP High	3.1	+ + +	+ + +	+ + + (rapid)	+ + +

EEG electroencephalogram, *DFP low* low responder, *DFP High* high responder

+ indicates a significant increase from baseline with increasing number of "+" symbols indicating increasing magnitude of difference from baseline; – indicates no change from baseline

inhibition presumed to be necessary for seizure initiation (Tonduli et al. 2001). We confirmed the lack of seizure activity in the DFP low responder subpopulation over the first 24 h post-exposure using both behavioral and EEG criteria. Consistent with previous reports of rats acutely intoxicated with DFP (Deshpande et al. 2010; Guignet et al. 2019) or soman (Prager et al. 2013), animals that did not exhibit seizure behavior were also negative for electrographic seizure activity. The level of AChE inhibition observed in three different brain regions associated with seizure initiation and propagation was comparable in DFP low vs. high responders, suggesting that the differential seizure responses are not due to differences in DFP distribution in the brain. It seems unlikely that AChE was significantly inhibited in DFP low responders in a brain region we did not examine because DFP is lipid soluble and rapidly penetrates all regions of the brain (Martin 1985). Moreover, it has been previously reported that acute intoxication of rats with a seizurogenic dose of DFP results in similar levels of AChE inhibition across multiple brain regions (Ferchmin et al. 2014).

While our study did not delineate mechanism(s) contributing to the seizure resistance of the DFP low responders, our observations are consistent with a report demonstrating that Sprague Dawley rats, which are an outbred strain, exhibit more variable seizure thresholds than inbred rat strains (Loscher et al. 2017). Indeed, previous studies have established that genetic background influences individual susceptibility to chemical convulsants in mice, rats, and non-human primates (Copping et al. 2019; Lin et al. 2012; Matson et al. 2017). Genetic mutations in α4 and β2 neuronal nicotinic acetylcholine receptor subunits are implicated as determinants of seizure susceptibility in rodent models, and mutations in the Kir4.1 gene, *Kcnj10*, have been linked to both rodent and human forms of epilepsy (Loscher et al. 2017). Whether these mutations contribute to the differential susceptibility of DFP low vs. high responder subpopulations is a testable hypothesis. Alternatively, it may be that DFP low responders are differentially responsive to the protective effects of atropine and/or oxime. However, that seems unlikely because both compounds are poorly brain penetrant and primarily protect against lethality by mitigating peripheral cholinergic symptoms (Bruun et al. 2019). A previous transcriptomic analysis of brains from seizing vs. non-seizing animals in a rat model of acute sarin intoxication identified increased expression of anti-inflammatory and apoptotic genes in the brains of non-seizing animals, suggesting that seizure resistance may be linked to differential activation of these pathways (Te et al. 2015).

While the DFP low responders were resistant to OP-induced seizures, this did not translate into protection against the neuropathological consequences associated with acute OP intoxication. The spatiotemporal pattern of neurodegeneration observed in the DFP high responders is consistent with previous studies of acute DFP (Li et al. 2011; Siso et al. 2017) and soman (McDonough and Shih 1997) intoxication. Also consistent with prior literature (McDonough and Shih 1997; Tanaka et al. 1996), the extent of neurodegeneration was positively correlated with seizure severity as reflected by the fact that DFP high responders exhibited earlier onset and greater magnitude of neurodegeneration compared to DFP low responders across all the brain regions and post-exposure times that were examined. Collectively, these finding suggest that while there is a positive correlation between seizure severity and the extent of neuronal damage, seizure activity is not the sole pathogenic mechanism responsible for neurodegeneration following acute OP intoxication.

The mechanism(s) contributing to neurodegeneration independent of sustained seizure activity in the DFP low responders remain unknown. In the rat model of acute soman intoxication, the resolution of neurodegeneration coincides temporally with the recovery of AChE (Prager et al. 2014), suggesting the possibility that persistent AChE inhibition contributes to the neurodegeneration observed in DFP low responders. However, the onset of neurodegeneration in the DFP low responders was delayed relative to the DFP high responders despite the fact that AChE inhibition was comparable in terms of both the level and timing of inhibition. This suggests that mechanisms other than or in addition to AChE inhibition are driving the neuropathology observed in the DFP low responders. Reports that OPs interact with multiple molecular targets in addition to AChE (reviewed in Terry 2012) support this possibility.

Additional alternative mechanisms driving DFP-induced neuropathology include neuroinflammation, (Banks and Lein 2012; Guignet and Lein 2019), oxidative stress, and disruption of axonal transport (Naughton and Terry 2018; Terry 2012; Zaja-Milatovic et al. 2009), all of which can be induced by exposure to OPs at levels that do not trigger seizures. Another possible mechanism suggested by the micro-CT data from this study is calcium dyshomeostasis. Calcium is a major constituent of mineralized regions in the brain commonly detected in the thalamus under various chronic neurological conditions (Valdes Hernandez Mdel et al. 2012). Published data support the hypothesis that calcium dyshomeostasis not only mediates acute excitotoxic neuronal injury, but also contributes to several comorbidities observed in survivors of acute OP intoxication, including cognitive dysfunction and acquired epilepsy (Deshpande et al. 2016). Thus, it has been proposed that calcium-stabilizing drugs may be effective neuroprotectants following acute OP intoxication (Deshpande et al. 2016). Our data demonstrating significant mineralization in the brains of non-seizing animals acutely intoxicated with DFP indicate that calcium-stabilizing drugs may be useful in treating not only OP-intoxicated individuals with SE, but also those with minimal evidence of seizure activity.

In summary, our findings imply that even if seizures do not occur, neuroprotective therapeutics may still be needed for individuals acutely intoxicated with OPs. Further study of animals that do not exhibit seizures in response to acute OP intoxication may identify mechanisms that confer resistance to OP-induced seizures and seizure-independent mechanisms that contribute to OP-induced neuropathology, thereby providing insight into novel therapeutic targets.

Acknowledgements We thank Dr. Suzette Smiley-Jewell (UC Davis CounterACT Center) for her assistance in editing this manuscript. This work was supported by the CounterACT Program, National Institutes of Health Office of the Director and the National Institute of Neurological Disorders and Stroke [grant number U54 NS079202], predoctoral fellowships to E.A.G from the National Institute of Neurological Disorders and Stroke [grant number F31 NS110522] and the National Institutes of Health Initiative for Maximizing Student Development [grant number R25 GM5676520], and predoctoral fellowships to M.G. from the National Institute of General Medical Sciences [grant number T32 GM099608], and the David and Dana Loury Foundation. This project used core facilities supported by the UC Davis MIND Institute Intellectual and Developmental Disabilities Research Center (U54 HD079125). The sponsors were not involved in the study design, in the collection, analysis, or interpretation of data, in the writing of the report, or in the decision to submit the paper for publication.

Author contributions EG: Conceptualization, Methodology, Investigation, Writing-Original Draft, Visualization. AR: Conceptualization, Methodology, Investigation, Writing-Original Draft. MG: Methodology, Investigation, Writing-Review and Editing, Visualization. JC: Methodology, Investigation, Visualization. DB: Conceptualization, Investigation, Supervision, Data Curation. AD: Methodology, Investigation. PA: Investigation. NS: Formal Analysis, Writing-Review and Editing, Visualization. DR: Methodology, Investigation, Data Curation, Writing-Review and Editing. DH: Formal Analysis, Writing-Original Draft, Visualization. MR: Funding Acquisition. PL: Conceptualization, Writing-Review and Editing, Supervision, Project Administration, Funding Acquisition.

Compliance with ethical standards

Conflict of interest The authors declare that they have no conflict of interest.

Ethical standards The authors certify that all animal experiments were performed in accordance with protocols approved by the UC Davis Institutional Animal Care and Use Committee (IACUC protocols #20122 and #20165), the ARRIVE guidelines, and the National Institutes of Health guide for the care and use of laboratory animals (NIH publication No. 8023, revised 1978). This article does not contain clinical studies or patient data.

References

Aggarwal M, Li X, Grohn O, Sierra A (2018) Nuclei-specific deposits of iron and calcium in the rat thalamus after status epilepticus revealed with quantitative susceptibility mapping (QSM). J Magn Reson Imaging 47:554–564. https://doi.org/10.1002/jmri.25777

Banks CN, Lein PJ (2012) A review of experimental evidence linking neurotoxic organophosphorus compounds and inflammation. Neurotoxicology 33:575–584. https://doi.org/10.1016/j.neuro.2012.02.002

Bruun DA, Guignet M, Harvey DJ, Lein PJ (2019) Pretreatment with pyridostigmine bromide has no effect on seizure behavior or 24 hour survival in the rat model of acute diisopropylfluorophosphate intoxication. Neurotoxicology 73:81–84. https://doi.org/10.1016/j.neuro.2019.03.001

Chen Y (2012) Organophosphate-induced brain damage: mechanisms, neuropsychiatric and neurological consequences, and potential therapeutic strategies. Neurotoxicology 33:391–400. https://doi.org/10.1016/j.neuro.2012.03.011

Copping NA, Adhikari A, Petkova SP, Silverman JL (2019) Genetic backgrounds have unique seizure response profiles and behavioral outcomes following convulsant administration. Epilepsy Behav 101:106547. https://doi.org/10.1016/j.yebeh.2019.106547

de Araujo FM, Rossetti F, Chanda S, Yourick D (2012) Exposure to nerve agents: from status epilepticus to neuroinflammation, brain damage, neurogenesis and epilepsy. Neurotoxicology 33:1476–1490. https://doi.org/10.1016/j.neuro.2012.09.001

Deshpande LS, Carter DS, Blair RE, DeLorenzo RJ (2010) Development of a prolonged calcium plateau in hippocampal neurons in rats surviving status epilepticus induced by the organophosphate diisopropylfluorophosphate. Toxicol Sci 116:623–631. https://doi.org/10.1093/toxsci/kfq157

Deshpande LS, Blair RE, Phillips KF, DeLorenzo RJ (2016) Role of the calcium plateau in neuronal injury and behavioral morbidities following organophosphate intoxication. Ann N Y Acad Sci 1374:176–183. https://doi.org/10.1111/nyas.13122

Ellman GL, Courtney KD, Andres V Jr, Feather-Stone RM (1961) A new and rapid colorimetric determination of acetylcholinesterase activity. Biochem Pharmacol 7:88–95

Ferchmin PA et al (2014) 4R-cembranoid protects against diisopropylfluorophosphate-mediated neurodegeneration. Neurotoxicology 44:80–90. https://doi.org/10.1016/j.neuro.2014.06.001

Flannery BM et al (2016) Persistent neuroinflammation and cognitive impairment in a rat model of acute diisopropylfluorophosphate intoxication. J Neuroinflam 13:267. https://doi.org/10.1186/s12974-016-0744-y

Gao J et al (2016) Diisopropylfluorophosphate impairs the transport of membrane-bound organelles in rat cortical axons. J Pharmacol Exp Ther 356:645–655. https://doi.org/10.1124/jpet.115.230839

Gayoso MJ, Al-Majdalawi A, Garrosa M, Calvo B, Diaz-Flores L (2003) Selective calcification of rat brain lesions caused by systemic administration of kainic acid. Histol Histopathol 18:855–869. https://doi.org/10.14670/HH-18.855

Guignet M, Lein PJ (2019) Organophopshates. In: Aschner M, Costa LG (eds) Advances in neurotoxicology: role of inflammation in environmental neurotoxicity. Academic Press, Cambridge, pp 35–79

Guignet M et al (2019) Persistent behavior deficits, neuroinflammation, and oxidative stress in a rat model of acute organophosphate intoxication. Neurobiol Dis. https://doi.org/10.1016/j.nbd.2019.03.019

Gunnell D, Eddleston M, Phillips MR, Konradsen F (2007) The global distribution of fatal pesticide self-poisoning: Systematic review. BMC Public Health 7:357. https://doi.org/10.1186/1471-2458-7-357

Heiss DR, Zehnder DW, Jett DA, Platoff GE, Yeung DT, Brewer BN (2016) Synthesis and storage stability of diisopropylfluorophosphate. Journal of Chemistry 2016:5. https://doi.org/10.1155/2016/3190891

Hernandez Mdel CV, Maconick LC, Tan EM, Wardlaw JM (2012) Identification of mineral deposits in the brain on radiological images: a systematic review. Eur Radiol 22:2371–2381. https://doi.org/10.1007/s00330-012-2494-2

Hobson BA, Rowland DJ, Supasai S, Harvey DJ, Lein PJ, Garbow JR (2017) A magnetic resonance imaging study of early brain injury

in a rat model of acute DFP intoxication. Neurotoxicology. https://doi.org/10.1016/j.neuro.2017.11.009
Lewine JD et al (2018) Addition of ketamine to standard-of-care countermeasures for acute organophosphate poisoning improves neurobiological outcomes. Neurotoxicology 69:37–46. https://doi.org/10.1016/j.neuro.2018.08.011
Li Y, Lein PJ, Liu C, Bruun DA, Tewolde T, Ford G, Ford BD (2011) Spatiotemporal pattern of neuronal injury induced by DFP in rats: a model for delayed neuronal cell death following acute OP intoxication. Toxicol Appl Pharmacol 253:261–269. https://doi.org/10.1016/j.taap.2011.03.026
Lin T, Duek O, Dori A, Kofman O (2012) Differential long term effects of early diisopropylfluorophosphate exposure in Balb/C and C57Bl/J6 mice. Int J Dev Neurosci 30:113–120. https://doi.org/10.1016/j.ijdevneu.2011.12.004
Loscher W, Ferland RJ, Ferraro TN (2017) The relevance of inter- and intrastrain differences in mice and rats and their implications for models of seizures and epilepsy. Epilepsy Behav 73:214–235. https://doi.org/10.1016/j.yebeh.2017.05.040
Martin BR (1985) Biodisposition of [3H]diisopropylfluorophosphate in mice. Toxicol Appl Pharmacol 77:275–284
Matson LM, McCarren HS, Cadieux CL, Cerasoli DM, McDonough JH (2017) The role of genetic background in susceptibility to chemical warfare nerve agents across rodent and non-human primate models. Toxicology 393:51–61. https://doi.org/10.1016/j.tox.2017.11.003
McDonough JH Jr, Shih TM (1997) Neuropharmacological mechanisms of nerve agent-induced seizure and neuropathology. Neurosci Biobehav Rev 21:559–579
McDonough JH Jr, Dochterman LW, Smith CD, Shih TM (1995) Protection against nerve agent-induced neuropathology, but not cardiac pathology, is associated with the anticonvulsant action of drug treatment. Neurotoxicology 16:123–132
Naughton SX, Terry AV Jr (2018) Neurotoxicity in acute and repeated organophosphate exposure. Toxicology 408:101–112. https://doi.org/10.1016/j.tox.2018.08.011
Okumura T et al (1996) Report on 640 victims of the Tokyo subway sarin attack. Ann Emerg Med 28:129–135. https://doi.org/10.1016/S0196-0644(96)70052-5
Okumura T et al (2005) Acute and chronic effects of sarin exposure from the Tokyo subway incident. Environ Toxicol Pharmacol 19:447–450. https://doi.org/10.1016/j.etap.2004.12.005
Peter JV, Sudarsan TI, Moran JL (2014) Clinical features of organophosphate poisoning: a review of different classification systems and approaches. Indian J Crit Care Med 18:735–745. https://doi.org/10.4103/0972-5229.144017
Phillips KF, Deshpande LS (2016) Repeated low-dose organophosphate DFP exposure leads to the development of depression and cognitive impairment in a rat model of Gulf War Illness. Neurotoxicology 52:127–133. https://doi.org/10.1016/j.neuro.2015.11.014
Pouliot W, Bealer SL, Roach B, Dudek FE (2016) A rodent model of human organophosphate exposure producing status epilepticus and neuropathology. Neurotoxicology 56:196–203. https://doi.org/10.1016/j.neuro.2016.08.002
Prager EM, Aroniadou-Anderjaska V, Almeida-Suhett CP, Figueiredo TH, Apland JP, Braga MF (2013) Acetylcholinesterase inhibition in the basolateral amygdala plays a key role in the induction of status epilepticus after soman exposure. Neurotoxicology 38:84–90. https://doi.org/10.1016/j.neuro.2013.06.006
Prager EM et al (2014) The recovery of acetylcholinesterase activity and the progression of neuropathological and pathophysiological alterations in the rat basolateral amygdala after soman-induced status epilepticus: relation to anxiety-like behavior. Neuropharmacology 81:64–74. https://doi.org/10.1016/j.neuropharm.2014.01.035
Russell RW, Overstreet DH, Messenger M, Helps SC (1982) Selective breeding for sensitivity to DFP: generalization of effects beyond criterion variables. Pharmacol Biochem Behav 17:885–891. https://doi.org/10.1016/0091-3057(82)90466-X
Siso S, Hobson BA, Harvey DJ, Bruun DA, Rowland DJ, Garbow JR, Lein PJ (2017) Editor's highlight: spatiotemporal progression and remission of lesions in the rat brain following acute intoxication with diisopropylfluorophosphate. Toxicol Sci 157:330–341. https://doi.org/10.1093/toxsci/kfx048
Tanaka K, Graham SH, Simon RP (1996) The role of excitatory neurotransmitters in seizure-induced neuronal injury in rats. Brain Res 737:59–63. https://doi.org/10.1016/0006-8993(96)00658-0
Te JA, Spradling-Reeves KD, Dillman JF 3rd, Wallqvist A (2015) Neuroprotective mechanisms activated in non-seizing rats exposed to sarin. Brain Res 1618:136–148. https://doi.org/10.1016/j.brainres.2015.05.034
Terry AV Jr (2012) Functional consequences of repeated organophosphate exposure: potential non-cholinergic mechanisms. Pharmacol Ther 134:355–365. https://doi.org/10.1016/j.pharmthera.2012.03.001
Thiermann H, Worek F, Kehe K (2013) Limitations and challenges in treatment of acute chemical warfare agent poisoning. Chem Biol Interact 206:435–443. https://doi.org/10.1016/j.cbi.2013.09.015
Todorovic MS, Cowan ML, Balint CA, Sun C, Kapur J (2012) Characterization of status epilepticus induced by two organophosphates in rats. Epilepsy Res 101:268–276. https://doi.org/10.1016/j.eplepsyres.2012.04.014
Tonduli LS, Testylier G, Masqueliez C, Lallement G, Monmaur P (2001) Effects of Huperzine used as pre-treatment against soman-induced seizures. Neurotoxicology 22:29–37
Yanagisawa N, Morita H, Nakajima T (2006) Sarin experiences in Japan: acute toxicity and long-term effects. J Neurol Sci 249:76–85. https://doi.org/10.1016/j.jns.2006.06.007
Zaja-Milatovic S, Gupta RC, Aschner M, Milatovic D (2009) Protection of DFP-induced oxidative damage and neurodegeneration by antioxidants and NMDA receptor antagonist. Toxicol Appl Pharmacol 240:124–131. https://doi.org/10.1016/j.taap.2009.07.006